Reduction of seizures by transplantation of cortical GABAergic interneuron precursors into Kv1.1 mutant mice

Scott C. Baraban[a,b,c,1], Derek G. Southwell[a,b,c,2], Rosanne C. Estrada[a,c,2] Daniel L. Jones[a,b], Joy Y. Sebe[a], Clara Alfaro-Cervello[d], Jose M. García-Verdugo[d], John L. R. Rubenstein[b,c,e] and Arturo Alvarez-Buylla[a,b,c]

Departments of [a]Neurological Surgery and [e]Psychiatry, [b]Program in Neuroscience, and [c]The Eli and Edythe Broad Center of Regeneration Medicine and Stem Cell Research, University of California, San Francisco, CA 94143; and [d]Instituto Cavanilles, Universidad de Valencia and Centro de Investigación Príncipe Felipe, 46013 Valencia, Spain

Epilepsy, a disease characterized by abnormal brain activity, is a disabling and potentially life-threatening condition for nearly 1% of the world population. Unfortunately, modulation of brain excitability using available antiepileptic drugs can have serious side effects, especially in the developing brain, and some patients can only be improved by surgical removal of brain regions containing the seizure focus. Here, we show that bilateral transplantation of precursor cells from the embryonic medial ganglionic eminence (MGE) into early postnatal neocortex generates mature GABAergic interneurons in the host brain. In mice receiving MGE cell grafts, GABA-mediated synaptic and extrasynaptic inhibition onto host brain pyramidal neurons is significantly increased. Bilateral MGE cell grafts in epileptic mice lacking a Shaker-like potassium channel (a gene mutated in one form of human epilepsy) resulted in significant reductions in the duration and frequency of spontaneous electrographic seizures. Our findings suggest that MGE-derived interneurons could be used to ameliorate abnormal excitability and possibly act as an effective strategy in the treatment of epilepsy.

epilepsy | inhibition | neocortex | therapy | graft

Epilepsy is a common neurological disorder characterized by abnormal electrical discharge, seizures, and loss of consciousness. Current antiepileptic drugs, which primarily target neurotransmitter receptors and ion channels, can be effective in suppressing seizures. However, prolonged drug treatment can have serious side effects, and some patients remain pharmacoresistant, requiring surgical resection of portions of the temporal lobe or other brain regions. Whether cell transplantation can be developed as an alternative therapeutic intervention for epilepsy requires investigation. Transplantation into the substantia nigra or hippocampus has resulted in modest suppression of evoked discharge; however, these studies did not demonstrate functional integration of transplanted cells within host circuits and did not provide evidence for a reduction of spontaneous electrographic seizures (1–4). Furthermore, prior transplantation strategies did not focus on generation of a specific cell type from grafted cells. Interneuron loss is a characteristic feature of the epileptic brain (5, 6), and genetically engineered cells that produce GABA, the primary inhibitory neurotransmitter in the mammalian nervous system, also attenuate seizure-like activity when transplanted into hippocampal and cortical sites (7–9). As such, a cell transplantation procedure to introduce functional cortical GABAergic neurons could be an effective strategy to reduce the abnormal electrical activity associated with epilepsy.

We have shown previously that unilateral, early postnatal embryonic medial ganglionic eminence (MGE) precursor cell transplants disperse widely and differentiate into functional GABAergic interneurons in the adult mouse brain (10, 11). Here, we used bilateral transplantation of MGE precursors in neonates to begin to establish a therapeutically relevant cell transplantation protocol that would broadly distribute interneurons in the host cortex. The cortical integration of MGE-derived cells was confirmed by using immunohistochemistry, slice electrophysiology, and electron microscopy. Reduction of abnormal electrical discharge after MGE cell transplantation in a mouse model of epilepsy was evaluated by using video EEG.

Results

New Cortical Interneurons After Bilateral MGE Cell Transplantation in the Postnatal Brain. MGE cells were harvested from mouse embryos expressing green fluorescent protein (GFP) and grafted into neonatal CD1 recipient mice. Thirty days after transplantation (DAT), grafted cells had dispersed in the postnatal cortex and expressed interneuron markers [GABA, GAD67, calretinin (CR), parvalbumin (PV), neuropeptide Y (NPY), or somatostatin (SOM); Fig. 1 *A* and *B*]. PV$^+$ and SOM$^+$ cells comprised the largest proportion of colabeled GFP$^+$ cells, as reported previously for MGE-derived interneurons (10). In neocortical tissue slices from grafted animals (30–40 DAT), MGE-GFP$^+$ neurons exhibited firing properties similar to three described classes of endogenous interneuron subtypes (12): (*i*) fast-spiking, (*ii*) regular-spiking nonpyramidal cells, and (*iii*) stuttering (Fig. 1 *C* and *D*). Consistent with previous observations (10, 11), graft-derived cells had immature and "migratory" anatomical profiles for the first week after transplantation. At 7–10 DAT, GFP$^+$ neurons showed immature intrinsic membrane properties; e.g., small and broad action potentials, depolarized resting membrane potential, and high input resistance (data not shown)

Selective Enhancement of Cortical Inhibition After MGE Cell Grafting. To assess levels of cortical inhibition in mice receiving early postnatal MGE cell grafts, we studied GABA-mediated input to endogenous pyramidal neurons by analysis of inhibitory postsynaptic current (IPSC). To isolate GABA-mediated currents, cells were voltage-clamped in a solution containing glutamate receptor antagonists [20 μM 6,7-dinitroquinoxaline-2,3-dione (DNQX) and 50 μM D-(-)-2-amino-5-phosphonovaleric acid (D-APV) or 3 mM kynurenic acid]. GABA-mediated events were abolished by addition of bicuculline (10 μM) or SR95331 (100 μM), confirming a role for postsynaptic GABA receptors. In acute cortical slices (300 μm thick; 30–40 DAT) with visible GFP$^+$ somata (3–10 cells per field of view; 40$\times$ objective), we measured a significant increase in IPSC
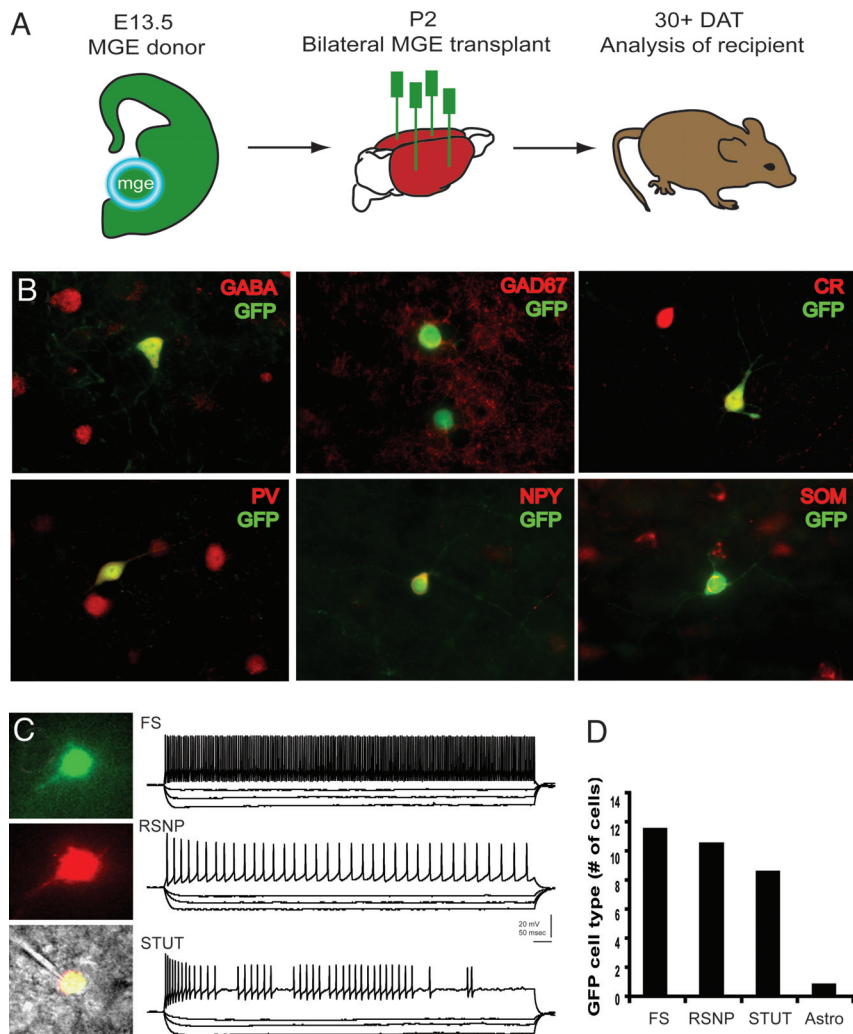
Fig. 1. Generation of interneurons from MGE precursors. (*A*) Schematic for MGE dissection (encircled region from GFP-expressing mouse embryos), bilateral transplantation into neonatal (P2) CD1 mice, and analysis at 30 DAT. (*B*) Immunohistochemical coexpression of GFP$^+$ cells with GABA, GAD67, CR, PV, NPY, and SOM. Representative cortical neurons are shown at 30 DAT. (*C*) Representative in vitro recording from a GFP$^+$ neuron in somatosensory cortex. (*Top*) Visualized patch-clamp recording from a GFP$^+$ cell identified under epifluorescence. (*Middle*) GFP$^+$ cell was filled with Alexa red via the patch pipette. (*Bottom*) Fluorescent images merged with IR-DIC image. Shown are sample current-clamp traces during depolarizing and hyperpolarizing steps to classify cells as fast-spiking (FS), regular-spiking nonpyramidal (RSNP), and stuttering (STUT) interneurons. (*D*) Summary plot for all GFP$^+$ cells recorded in current-clamp at 30–40 DAT. Note: one cell classified as a putative astrocyte exhibited a hyperpolarized resting membrane potential and failed to generate action potentials upon depolarization.

mean frequency onto host pyramidal neurons in layer II/III ($n = 20$; Fig. 2 *A* and *Bi*) compared with endogenous pyramidal neurons in two types of age-matched CD1 wild-type controls: (*i*) vehicle-injected ($n = 11$) or (*ii*) mice receiving "dead" freeze–thawed cells ($n = 7$). All IPSC parameters (e.g., frequency, amplitude, decay or rise time) among the two control groups were statistically indistinguishable, and they were therefore pooled into one group (Fig. 2 *Bii*–*Biv*).

Because MGE precursors may also generate interneurons that innervate endogenous interneurons, possibly leading to increased excitation, we determined whether GABA-mediated inhibition onto host interneurons was enhanced. We examined IPSCs on interneurons in acute cortical slices with visible GFP-positive somata; in some cases, these slices were adjacent to those used for pyramidal cell IPSC analysis. Host interneurons were identified as GFP-negative cells that, under infrared differential interference contrast (IR-DIC) visualization, had oval, often multipolar morphologies; this was confirmed post hoc with biocytin labeling (data not shown). Comparison of control ($n = 21$) and grafted ($n = 21$) mice at 30–40 DAT showed that MGE transplantation did not

produce a significant alteration of IPSC properties recorded from host interneurons (Fig. 3).

To examine whether new inhibitory synapses with distinct kinetics are preferentially located at a specific electrotonic distance from the somatic recording electrode, we constructed cumulative histograms for IPSC amplitude and decay time (Fig. S1). The amplitude histograms for sIPSCs recorded from pyramidal neurons (Fig. S1*A1*) or interneurons (Fig. S1*A2*) in grafted mice did not reveal any "new" peaks relative to controls. The same was true for decay-time histograms recorded from pyramidal cells (Fig. S1*B1*) or interneurons (Fig. S1*B2*) in control vs. grafted mice (Kolmogorov–Smirnov test, $P > 0.05$). As expected, given the selective increase in IPSC frequency recorded from pyramidal cells (Fig. 2), but not interneurons (Fig. 3), the frequency distributions of IPSC amplitudes recorded from pyramidal cells in control and grafted mice are statistically different (Kolmogorov–Smirnov test, $P < 0.05$).

To further examine inhibition in the host brain, we studied tonic inhibition onto host pyramidal neurons in layer II/III (Fig. 4) by using the same recording parameters described above. To measure
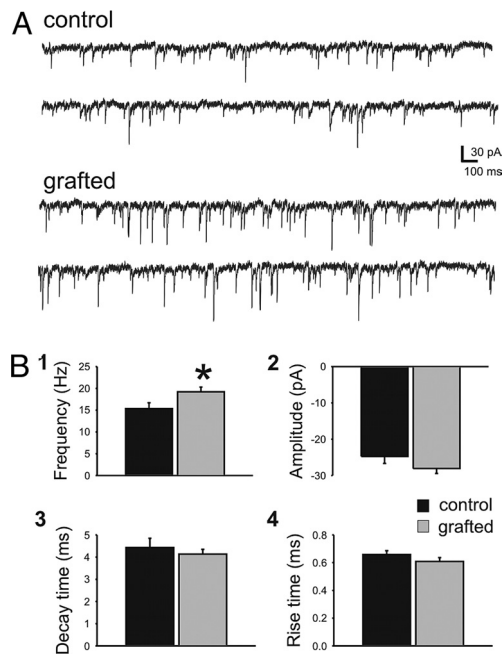
NEUROSCIENCE

Fig. 2. MGE cell grafting increased inhibitory input onto host pyramidal cells. Spontaneous IPSCs were recorded from endogenous pyramidal cells near GFP$^+$ cells in neocortex. (*A*) Representative voltage-clamp recordings from endogenous pyramidal cells in vehicle-treated control (*Upper*) and MGE-grafted (*Lower*) neocortical slices. (*B*) Summary bar plots for sIPSC frequency (*Bi*), amplitude (*Bii*), decay time (*Biii*), and rise time (*Biv*). sIPSC frequency recorded from pyramidal cells increased relative to controls by 25% from 15 ± 1 Hz (control) to 19 ± 1 Hz (grafted). There was no statistically significant difference in the amplitude, decay time, or rise times between control and grafted mice. Data are shown as mean ± SEM. *, $P < 0.05$; unpaired t test.
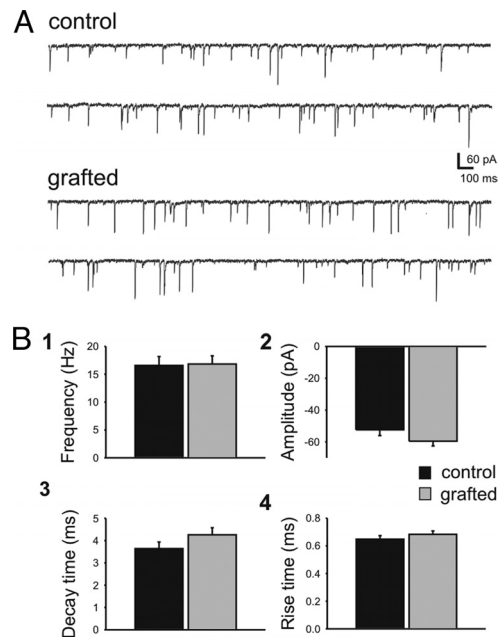

Fig. 3. MGE cell grafting did not increase inhibitory input onto host interneurons. Spontaneous IPSCs were recorded from endogenous interneurons near GFP$^+$ cells in neocortex. (*A*) Representative voltage-clamp recordings from endogenous interneurons in vehicle-treated control (*Upper*) and MGE-grafted (*Lower*) neocortical slices. Note that the electrical noise appears smaller in Fig. 3 (compared with Fig. 2) because the trace has been scaled down by a factor of 2 to show the larger-amplitude events. (*B*) Summary bar plots for sIPSC frequency (*Bi*), amplitude (*Bii*), decay time (*Biii*), and rise time (*Biv*). sIPSC frequency recorded from host interneurons in control (17 ± 1 Hz) and grafted (17 ± 2 Hz) mice was unchanged. There was no statistically significant difference in the amplitude, decay time, or rise times between control and grafted mice. Data are shown as mean ± SEM.

tonic currents due to endogenous GABA, we blocked the GABA transporters GAT1 and GAT2/3 via bath application of NO711 (20 μM) and SNAP-5114 (100 μM), respectively, followed by gabazine (100 μM). Pyramidal cells from grafted mice exhibited a significant increase in mean tonic current (Fig. 4*C*); no difference in the percent change in the SD between control (−55% ± 12%; $n = 22$) and grafted (−62% ± 24%; $n = 21$) mice was noted. Finally, ultrastructural analysis shows that MGE-derived, GFP-positive interneurons received input from host brain neurons (Fig. 5*A*). GFP-positive cells also established synaptic contact onto the dendrites of unlabeled, presumably host brain neurons (Fig. 5*B*); GFP–GFP contacts were not observed. Electrophysiological data suggest that the graft-derived interneurons primarily target excitatory pyramidal neurons. This is consistent with the enhancement of GABA-mediated inhibition observed in the present study and following unilateral grafts (10).

Suppression of Spontaneous Seizures After MGE Cell Grafting. Given that many antiepileptic drugs (AEDs) function via enhancement of GABA-mediated synaptic transmission (13), and interneuron loss is a feature of the epileptic brain (5, 6), we examined whether MGE-derived interneurons modify seizures in an animal model of epilepsy. We chose a mouse loss-of-function mutant of a Shaker-like potassium channel (*Kv1.1/Kcna1*) (14) that mimics a neuronal ion channelopathy associated with epilepsy in humans (15). The seizure phenotype of $Kv1.1^{-/-}$ mutant mice is severe and begins during the second to third postnatal weeks. To monitor spontaneous tonic-clonic seizures, we performed prolonged video EEG starting around P32, or ≈30 DAT (see *Materials and Methods* for full description of electrographic phenotypes). As expected (14, 16, 17), the EEG of Kv1.1$^{-/-}$ mice showed generalized electrographic seizures lasting between 10 and 340 seconds and occurring approx-

imately once per hour (Fig. 6*A*). In untreated ($n = 4$; P37–P39) or vehicle-injected ($n = 4$; P32–P38) Kv1.1$^{-/-}$ mice, electrographic seizures began with variable-frequency spikes (Fig. 6*Bi*), progressing through a period of high-frequency, high-voltage synchronized spiking (Fig. 6*Bii*), longer-duration polyspikes with phase-locked, high-frequency oscillations (Fig. 6*Biii*), large-amplitude spike and slow-wave discharges (Fig. 6*Biv*) and, finally, abrupt termination. Electrographic seizures or high-voltage spiking were never observed in age-matched wild-type controls ($n = 3$; P35–P38; data not shown). Simultaneous video monitoring at two different viewing angles confirmed tonic-clonic, Racine (18) stage 4 seizure behaviors (e.g., tonic arching and tail extension, followed by forelimb clonus, then synchronous forelimb–hindlimb clonus, rearing, and loss of posture) during these electrographic episodes. In contrast, age-matched Kv1.1$^{-/-}$ mice grafted with MGE cells bilaterally ($n = 8$; P32–P39) exhibited a significant reduction in electrographic seizure activity (Table S1). Brief episodes (10–48 sec) of synchronized high-voltage spiking and/or polyspike bursting were observed in Kv1.1$^{-/-}$ mice that underwent transplantation and were monitored beginning at 30 DAT (Fig. 6 *C* and *D*). Behaviors associated with electrographic events primarily consisted of myoclonic jerks or brief episodes of forelimb–hindlimb clonus. When they occurred, the duration of electrographic events was significantly shorter in MGE-grafted Kv1.1$^{-/-}$ mice compared with untreated or vehicle-injected mutants (Fig. 6*E* and Table S1), and the total number of electrographic seizures recorded in grafted animals was reduced by 86% (Fig. 6*F* and Table S1). A cumulative histogram of all recorded electrical seizure events confirms the higher number and longer duration in Kv1.1 mutants compared with MGE-grafted mice (Fig. 6*G*).

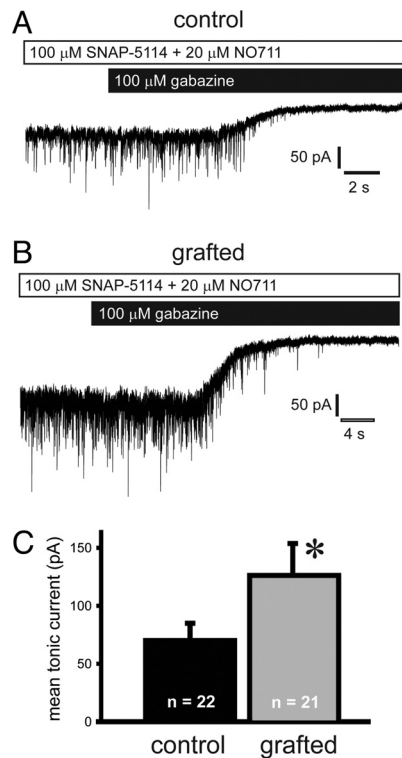All animals were killed at the conclusion of EEG monitoring and

Fig. 4. MGE cell grafting increased tonic current onto host pyramidal cells. Spontaneous IPSCs were recorded from endogenous pyramidal cells near GFP$^+$ cells in neocortex. (*A* and *B*) Representative voltage-clamp recordings from pyramidal cells in neocortical slices from a vehicle-treated control (*A*) or an MGE-grafted mouse (*B*). Slices were first bath-perfused with 20 μM DNQX, 25 μM APV, 20 μM NO711, and 100 μM SNAP-5114. To measure the tonic GABA current, the GABA$_A$ receptor antagonist gabazine (100 μM) was bath-applied. Application of gabazine abolished all synaptic events. (*C*) MGE cell grafting increased the mean tonic by 80%, from 70 $\pm$ 15 pA in control to 126 $\pm$ 28 pA in grafted mice. Data are shown as mean $\pm$ SEM. *, $P < 0.05$; unpaired t test.
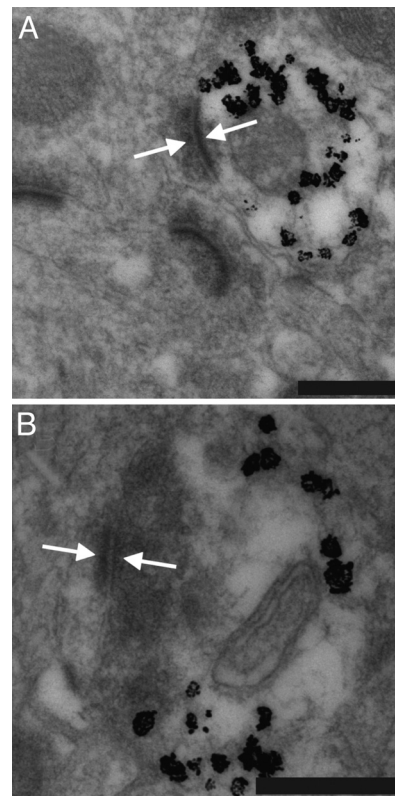

Fig. 5. Integration of MGE-derived interneurons in the host brain. (*A*) Transmission electron micrographs of transplanted neurons labeled with immunogold for GFP (silver-enhanced black granules). Grafted cells had medium-sized soma characteristic of GABAergic interneurons, with invaginated nuclei and sparse endoplasmic reticulum. GFP-labeled neurons receive synaptic contacts from unlabeled host neurons. (*B*) GFP-labeled neurons make synaptic contacts onto unlabeled host neurons. Arrows indicate synaptic densities in the labeled transplanted cell and unlabeled host cell. (Scale bars: 200 μm.)

processed for GFP and interneuron-marker immunohistochemistry ([Fig. S2](#)): GFP/GABA (64.8%), GFP/PV (29.2%), GFP/SOM (43.9%), GFP/NPY (9.5%), and GFP/CR (5.1%). Consistent with previously published data (12, 14, 15), a large percentage of Kv1.1$^{-/-}$ mice do not survive beyond 5–6 weeks after birth. Transplantation of MGE precursors resulted in a small, not statistically significant, increase in survival in animals reared under identical conditions. The mean survival ages for Kv1.1$^{-/-}$ mice grafted with MGE cells were 56 $\pm$ 3 days (range, 38–70 days; $n = 11$) and 49 $\pm$ 4 days (range, 25–69 days; $n = 9$; Student's t test $P = 0.16$) for vehicle-injected and "dead-cell" Kv1.1$^{-/-}$ controls.

Discussion

Transplantation of embryonic MGE interneuron precursors into the postnatal neocortex primarily generates cells that disperse and differentiate into interneurons of three functional subtypes. In mice receiving MGE cell grafts, we observed an enhancement of GABA-mediated inhibition onto host pyramidal neurons, suggesting they could be useful in conditions of excess excitation, such as epilepsy. Indeed, postnatal MGE cell grafts resulted in a significant reduction of spontaneous electrographic seizures in a rodent model of generalized epilepsy associated with a potassium-channel deletion. Given that transplantations were performed before the emergence of spontaneous seizures in these mice, this strategy could be classified as "antiepileptogenic."

Consistent with our previously published data (10), but under more physiologically relevant recording conditions, host brain regions containing MGE-derived GFP$^+$ cells exhibited an increased level of GABA-mediated synaptic activity compared with controls.

This conclusion is based on: (*i*) current-clamp and immunohistochemical data demonstrating that MGE-derived cells become functionally mature cortical interneurons; (*ii*) EM data showing synaptic contact between GFP$^+$ processes and host brain; (*iii*) physiological data demonstrating a significant increase in the frequency of sIPSCs onto host brain pyramidal neurons; and (*iv*) an enhancement of tonic currents in grafted animals. At the same time, we did not detect a significant alteration in GABA-mediated inhibition of host brain interneurons, suggesting that subclasses that selectively target other interneurons (e.g., bipolar calretinin-positive cells) are not generated in significant numbers from these grafts. Although new interneuron–interneuron synapses may form between grafted GFP$^+$ cells and the host brain neurons, this interneuron subclass is thought to derive from the caudal ganglionic eminence (12), whereas the transplanted cells derive from the MGE. Because the exact origin of the increased IPSCs has not been ascertained, paired recordings between endogenous and transplanted (GFP$^+$) interneurons will ultimately need to be performed to establish physiologically active synaptic contacts between grafted cells and the host brain.

Clinical application of neural transplantation therapies critically depends on whether grafted cells ameliorate disease symptoms. Prior attempts to use transplantation to modify stimulation-induced electrical afterdischarge demonstrated modest suppression by using: (*i*) immortalized cells engineered to produce GABA (7, 9), (*ii*) embryonic stem cells modified to release adenosine (4), (*iii*) fetal
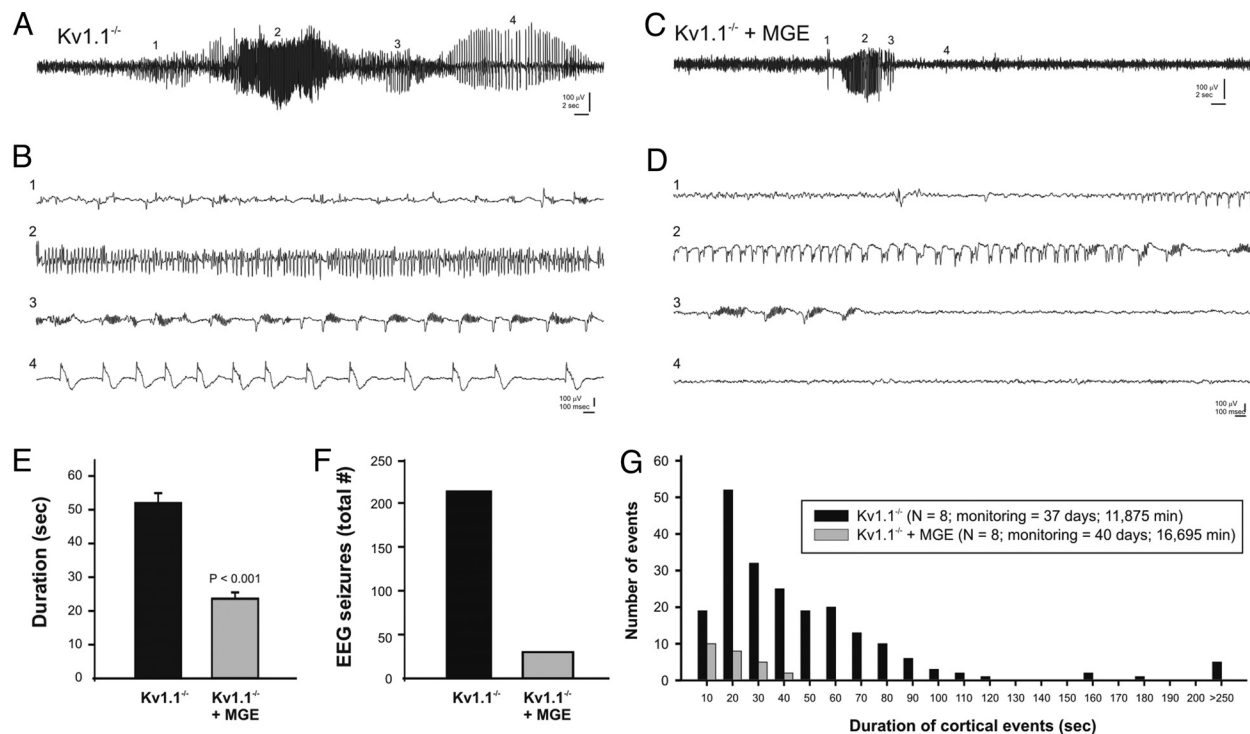
NEUROSCIENCE

Fig. 6. Seizure suppression in the Kv1.1 mouse model of epilepsy. (*A*) Sample EEG from a control vehicle-injected Kv1.1$^{-/-}$ mouse during a typical grade IV electrographic seizure. (*B*) The same seizure but with high resolution at four different stages of seizure progression (as noted by *i–iv*). (*C* and *D*) Sample EEG from Kv1.1$^{-/-}$ mouse grafted with MGE cells at P2. Note the seizure progression (*Di–Div*) is shorter. Summary bar plots show grade IV seizure duration (*E*) and the total number of seizures recorded (*F*). Data in *E* are shown as mean ± SEM. (*G*) Histogram showing durations for all electrographic seizures recorded in Kv1.1$^{-/-}$ (untreated, *n* = 4; vehicle-injected, *n* = 4; black bars) and Kv1.1$^{-/-}$ mice grafted with MGE cells (*n* = 8; gray bars). Total monitoring days and minutes are shown in the key. Given that control groups were monitored for a longer period (40 vs. 37 days; 16,695 vs. 11,875 min), it is possible that these results, which show a clear suppression of seizure activity, slightly overestimate the number of seizures occurring in grafted animals.

"GABA-rich" tissue (19, 20), or (*iv*) viral vectors engineered to produce glial cell line-derived neurotrophic factor (21), neuropeptide Y (22), or galanin (23, 24). In addition, a reduction in behavioral seizures in rat models of acquired epilepsy was observed after grafting of embryonic stem cells (25), striatal precursor cells (26), or fetal hippocampal cells (27). These cell transplantation procedures primarily transplanted into the substantia nigra or hippocampus, relied exclusively on assessment of stimulation-evoked afterdischarge or behavioral observation, and often showed only transient effects. Although promising in concept, none of these procedures demonstrated significant migration (or viral infection) of cells away from the injection site, substantial numbers of new GABAergic interneurons, evidence for selective modification of synaptic transmission in the host brain, or suppression of spontaneous, unprovoked, electrographic seizures (e.g., the hallmark feature of epilepsy).

Although interneuron loss has been reported in epilepsy (5, 6), and GABA-enhancing AEDs are used clinically (13), a procedure to modify host brain circuits via the introduction of new cortical interneurons has never been demonstrated successfully. Here, MGE cell grafts were shown to produce a striking reduction in electrographic seizure activity in Kv1.1 mutant mice. Seizures are generalized in these animals (14, 16), and we did not perform a treatment to introduce MGE precursors in all regions of the brain that are likely affected by the potassium-channel deficit. Note also that our grafting procedure was not designed to rescue the channel mutation; nonetheless, the effective dispersion of MGE-derived interneurons across a fairly wide region of neocortex (10) was shown to be sufficient to suppress abnormal electrical discharges and clinical characteristics of seizures in these animals. Our data are consistent with a longstanding hypothesis that synaptic inhibition constrains seizure discharge (28, 29). It remains to be established that this type of graft procedure does not result in unwanted behavioral side effects, or that grafts into adult brain can be effective after seizures emerge. In conclusion, our data suggest that MGE interneuron precursor transplantation could potentially serve as a cell-based therapeutic approach for human epilepsy.

Materials and Methods

Transplantation. Ventricular and subventricular layers of the MGE germinal region were dissected from embryonic day 13.5 embryonic GFP$^+$ transgenic mice, as described in ref. 10. Highly concentrated cell suspensions ($\approx$8 $\times$ 10^5 cells per microliter in 3–5 μL of L-15 medium) were front-loaded into beveled glass micropipettes ($\approx$50-μm diameter) prefilled with mineral oil and mounted on a microinjector for transplantation into anesthetized (on ice for 2.5 min) mouse pups (P1–P3). Bilateral injections ($\approx$4 $\times$ 10^5 cells per mouse) were made into deep layers of cortex at two different sites per hemisphere; sham-operated controls were injected with an equal volume of vehicle or freeze–thawed (three to four times) "dead" cells. Transplantations were considered successful if the density and migration of graft-derived GFP cells in the host brain were evenly distributed in both hemispheres and confirmed as ≥40,000 cells per cortex and ≥1 mm from the injection site; all criteria were met in all WT mice and some EEG-monitored animals. Transplantation success rates were $\approx$69% for CD1 and $\approx$65% for Kv1.1$^{-/-}$ mice.

Immunostaining. Animals were transcardially perfused with 4% paraformaldehyde and processed for immunohistochemistry, as described in ref. 10. Fluorescent images were obtained by using a cooled-CCD camera (Princeton Instruments) and Metamorph software (Universal Imaging).

Electron Microscopy. CD1 mice bilaterally injected with MGE-GFP cells at P2 were processed at 150 DAT. First, immunocytochemistry was performed on brains fixed in 4% paraformaldehyde and 0.5% glutaraldehyde, then postfixed in 4% paraformaldehyde. Sections (50 μm) were washed in 0.1 M phosphate buffer (PB), cryoprotected in 25% saccharose, and freeze–thawed (3$\times$) in methyl-butane and

dry ice. Sections were washed in PB, blocked in 0.3% BSA-C (BSA; Aurion), and incubated in primary chicken anti-GFP antibody (1:200 in PB for 3 days at 4 °C; Aves Laboratories). Sections were washed in PB, blocked in 0.5% BSA and 0.1% fish gelatin (1 h at room temperature), and incubated in colloidal gold-conjugated anti-chicken secondary antibody (1:50 for 24 h). Sections were washed in PB and 2% sodium acetate. Silver enhancement was performed (per Aurion instructions) and washed again in 2% sodium acetate. To stabilize silver particles, samples were immersed in 0.05% gold chloride (10 min at 4 °C), washed in sodium thiosulfate, and then washed in PB and postfixed in 2% glutaraldehyde (30 min). Sections were contrasted with 1% osmium and 7% glucose and embedded in araldite. Second, semithin 1.5-μm sections were prepared, selected at the light microscope level, and reembedded for ultrathin sectioning at 70 nm. Photomicrographs were obtained under a Fei microscope (Tecnai-Spirit) using a digital camera (Morada; Soft Imaging System).

Electrophysiology. Acute neocortical slices were prepared as described in ref. 10. For voltage-clamp recordings, intracellular patch solution contained (in mM): 140 CsCl$_2$, 10 Hepes, 11 EGTA, 1 MgCl$_2$, 1.25 QX314, 2 Na$_2$-ATP, and 0.5 Na$_2$-GTP (pH 7.25; 285–290 mOsm). To isolate GABA currents, slices were perfused with normal artificial cerebrospinal fluid containing 20 μM DNQX and 50 μM D-APV or 3 mM kynurenic acid. Slices were maintained at 33–34 °C, and cells were held at −60 mV (gain = 5; 1-kHz filter using amplifier). For current-clamp recordings, intracellular patch solution contained (in mM): 120 KMeGluconate, 10 KCl, 1 MgCl$_2$, 0.025 CaCl$_2$, 10 Hepes, 0.2 EGTA, 2 Mg-ATP, and 0.2 Na-GTP, pH 7.2 (285–290 mOsm). For analysis of intrinsic firing properties, recordings were obtained from GFP$^+$ cells in the neocortex identified on an IR-DIC microscope equipped with epifluorescence (Olympus America); cells were depolarized and hyperpolarized via direct current injection (5–1,000 ms, duration). Current and voltage were recorded with an Axopatch 1D amplifier (Axon Instruments) and monitored on an oscilloscope. Whole-cell access resistance was carefully monitored, and cells were rejected if values changed by >20%; only recordings with stable series resistance of <20 MΩ were used for IPSC analysis (at least 100 events per cell). IPSC data recorded from endogenous pyramidal cells and interneurons were coded and analyzed "blind" by using MiniAnalysis software (Synaptosoft). For all cells, decays of the average IPSC reported in Figs. 2 and 3 were fit to two exponentials, and a weighted decay-time constant was calculated. For decay-time histograms (Fig. S1), the decay time was defined as time to 50% (pyramidal) and 67% (interneuron) of peak. In all experiments, there was no difference between data acquired from male and female mice as assessed by unpaired t tests, so the data were pooled. Unpaired t tests ($P < 0.05$) were used to assess statistical differences in sIPSC frequency, amplitude, and decay time in control vs. grafted mice. Two sample Kolmogorov–Smirnov tests ($P < 0.05$) were used to examine changes in the amplitude and decay-time distributions.

Video EEG Monitoring. Behavioral and EEG observations were made by using a time-locked video EEG monitoring system (Pinnacle Technologies). For EEG recordings, mice were surgically implanted in the left and right frontoparietal cortex with electrodes. Each mouse was anesthetized with ketamine and xylazine (10 mg/kg and 1 mg/kg i.p., respectively) so that there was no limb-withdrawal response to a noxious foot pinch. Sterile, stainless steel bone screw recording electrodes were placed epidurally through burr holes in the skull (one electrode on either side of the sagittal suture, approximately halfway between bregman and lambdoid sutures and ≈1 mm from the midline). Electrodes were cemented in place with a fast-acting adhesive and dental acrylic, and electrode leads were attached to a microplug that was also cemented to the head of the animal. Animals were allowed to recover for 3–5 days before experiments were initiated.

Electrographic seizures (30) were defined as follows: grade I, basic background, no epileptiform spikes; grade II, mostly normal background, some high-voltage spikes; grade III, mostly abnormal background with low-frequency, high-voltage spiking; and grade IV, high-frequency, high voltage synchronized polyspike or paroxysmal sharp waves with amplitude >2-fold background that lasted ≥6 sec. Electrographic EEG seizures were analyzed by using SireniaScore software (Pinnacle) and confirmed by offline review of behavioral video recordings obtained at two different monitoring angles. Behavior was scored between stage 1 (S1) and S4 on a modified Racine scale (18). Experimental animals were monitored for 3–8 days (6–10 h/day; at least 20 h per animal). A total of 11,875 min (37 days) of recording were analyzed for Kv1.1$^{-/-}$ mice ($n = 8$) and 16,695 min (40 days) for Kv1.1$^{-/-}$ mice grafted with MGE cells ($n = 8$). Because electrographic seizure activities in untreated Kv1.1$^{-/-}$ and vehicle-injected sham Kv1.1$^{-/-}$ mice were comparable in duration (53.5 ± 4.3 sec vs. 49.1 ± 2.8 sec; $P = 0.92$), frequency (1.1 ± 0.4 seizures per hour vs. 0.9 ± 0.1 seizures per hour; $P = 0.64$), and severity (electrographic grade IV; Racine S4), the data from these two groups were pooled.

1. Shetty AK, Zaman V, Hattiangady B (2005) Repair of the injured adult hippocampus through graft-mediated modulation of the plasticity of the dentate gyrus in a rat model of temporal lobe epilepsy. *J Neurosci* 25:8391–8401.
2. Shetty AK, Hattiangady B (2007) Restoration of calbindin after fetal hippocampal CA3 cell grafting into the injured hippocampus in a rat model of temporal lobe epilepsy. *Hippocampus* 17:943–956.
3. Huber K, et al. (2001) Grafts of adenosine-releasing cells suppress seizures in kindling epilepsy. *Proc Natl Acad Sci USA* 98:7611–7616.
4. Li T, et al. (2007) Suppression of kindling epileptogenesis by adenosine releasing stem cell-derived brain implants. *Brain* 130:1276–1288.
5. de Lanerolle NC, Kim JH, Robbins RJ, Spencer DD (1989) Hippocampal interneuron loss and plasticity in human temporal lobe epilepsy. *Brain Res* 495:387–395.
6. Spreafico R, et al. (1998) Cortical dysplasia: An immunocytochemical study of three patients. *Neurology* 50:27–36.
7. Thompson K, et al. (2000) Conditionally immortalized cell lines, engineered to produce and release GABA, modulate the development of behavioral seizures. *Exp Neurol* 161:481–489.
8. Gernert M, Thompson KW, Löscher W, Tobin AJ (2002) Genetically engineered GABA-producing cells demonstrate anticonvulsant effects and long-term transgene expression when transplanted into the central piriform cortex of rats. *Exp Neurol* 176:183–192.
9. Thompson KW (2005) Genetically engineered cells with regulatable GABA production can affect afterdischarges and behavioral seizures after transplantation into the dentate gyrus. *Neuroscience* 133:1029–1037.
10. Alvarez-Dolado M, et al. (2006) Cortical inhibition modified by embryonic neural precursors grafted into the postnatal brain. *J Neurosci* 26:7380–7389.
11. Wichterle H, Garcia-Verdugo JM, Herrera DG, Alvarez-Buylla A (1999) Young neurons from medial ganglionic eminence disperse in adult and embryonic brain. *Nat Neurosci* 2:461–466.
12. Fishell G (2007) Perspectives on the developmental origins of cortical interneuron diversity. *Novartis Found Symp* 288:21–35.
13. Macdonald RL, McLean MJ (1986) Anticonvulsant drugs: Mechanisms of action. In: Delgado-Escueta AV, Ward AA, Woodbury DM, Porter RJ (eds), *Advances in Neurology: Basic Mechanisms of the Epilepsies. Molecular and Cellular Approaches* (Raven Press, New York), pp 713–736.
14. Smart SL, et al. (1998) Deletion of the K(V)1.1 potassium channel causes epilepsy in mice. *Neuron* 20:809–819.
15. Zuberi SM, et al. (1999) A novel mutation in the human voltage-gated potassium channel gene (Kv1.1) associates with episodic ataxia type 1 and sometimes with partial epilepsy. *Brain* 122:817–825.
16. Wenzel HJ, et al. (2007) Structural consequences of Kcna1 gene deletion and transfer in the mouse hippocampus. *Epilepsia* 48:2023–2046.
17. Glasscock E, Qian J, Yoo JW, Noebels JL (2007) Masking epilepsy by combining two epilepsy genes. *Nat Neurosci* 10:1554–1558.
18. Racine RJ (1972) Modification of seizure activity by electrical stimulation. II. Motor seizure. *Electroencephalogr Clin Neurophysiol* 32:281–294.
19. Fine A, Meldrum BS, Patel S (1990) Modulation of experimentally induced epilepsy by intracerebral grafts of fetal GABAergic neurons. *Neuropsychologia* 28:627–634.
20. Löscher W, Ebert U, Lehmann H, Rosenthal C, Nikkah G (1998) Seizure suppression in kindling epilepsy by grafts of fetal GABAergic neurons in rat substantia nigra. *J Neurosci Res* 51:196–209.
21. Kanter-Schlifke I, Georgievska B, Kirik D, Kokaia M (2007) Seizure suppression by GDNF gene therapy in animal models of epilepsy. *Mol Ther* 15:1106–1113.
22. Richichi C, et al. (2004) Anticonvulsant and antiepileptogenic effects mediated by adeno-associated virus vector neuropeptide Y expression in the rat hippocampus. *J Neurosci* 24:3051–3059.
23. Haberman P, Samulski RJ, McCown TJ (2003) Attenuation of seizures and neuronal death by adeno-associated virus vector galanin expression and secretion. *Nat Med* 9:1076–1080.
24. McCown TJ (2006) Adeno-associated virus-mediated expression and constitutive secretion of galanin suppresses limbic seizure activity in vivo. *Mol Ther* 14:63–69.
25. Carpentino JE, Hartman NW, Grabel LB, Naegele JR (2008) Region-specific differentiation of embryonic stem cell-derived neural progenitor transplants into the adult mouse hippocampus following seizures. *J Neurosci Res* 86:512–524.
26. Hattiangady B, Rao MS, Shetty AK (2008) Grafting of striatal precursor cells into hippocampus shortly after status epilepticus restrains chronic temporal lobe epilepsy. *Exp Neurol* 212:468–481.
27. Rao MS, et al. (2007) Strategies for promoting anti-seizure effects of hippocampal fetal cells grafted into the hippocampus of rats exhibiting chronic temporal lobe epilepsy. *Neurobiol Dis* 27:117–132.
28. Dichter M, Spencer WA (1969) Penicillin-induced interictal discharges from the cat hippocampus. II. Mechanisms underlying origin and restriction. *J Neurophysiol* 32:663–687.
29. Trevelyan AJ, Sussillo D, Watson BO, Yuste R (2006) Modular propagation of epileptiform activity: Evidence for an inhibitory veto in neocortex. *J Neurosci* 26:12447–12455.
30. Dubé C, et al. (2006) Temporal lobe epilepsy after experimental prolonged febrile seizures: Prospective analysis. *Brain* 129:911–922.

NEUROSCIENCE